

SRLM: Human-in-Loop Interactive Social Robot Navigation with Large Language Model and Deep Reinforcement Learning

Weizheng Wang¹, Le Mao¹, Ruiqi Wang¹, and Byung-Cheol Min¹

Abstract—An interactive social robotic assistant must provide services in complex and crowded spaces while adapting its behavior based on real-time human language commands or feedback. In this paper, we propose a novel hybrid approach called Social Robot Planner (SRLM), which integrates Large Language Models (LLM) and Deep Reinforcement Learning (DRL) to navigate through human-filled public spaces and provide multiple social services. SRLM infers global planning from human-in-loop commands in real-time, and encodes social information into a LLM-based large navigation model (LNM) for low-level motion execution. Moreover, a DRL-based planner is designed to maintain benchmarking performance, which is blended with LNM by a large feedback model (LFM) to address the instability of current text and LLM-driven LNM. Finally, SRLM demonstrates outstanding performance in extensive experiments. More details about this work are available at: <https://sites.google.com/view/navi-srlm>.

I. INTRODUCTION

Navigating in the human-filled spaces is a crucial aspect of social robots to support various of advanced services, such as cooperating or walking together with users. The socially-aware navigation (SAN) task faces two main challenges: the aspect of real-time highly volatile user requests or feelings, and the constraint of managing socially compliant or acceptable navigation behaviors within dynamic environments. With the developments in robotics and artificial intelligence technologies, current approaches have addressed the aforementioned issues to implement social robots in public environments [1]. These approaches are inspired by significant insights from fields such as machine learning [2], sociology [3], analytical mechanics [4], algebra and geometry [5], [6], and others.

However, both existing learning-based and conventional approaches exhibit limited adaptability when it comes to real-time response requirements. Therefore, we design an interactive Social Robot navigation Large Model (SRLM) that can infer and execute users' real-time commands, leveraging the promising potential of large language model (LLM) in human language understanding. For instance, users can adjust robot configuration or behavioral styles corresponding to personal feelings in real-time, a challenge that current state-of-the-art (SOTA) planners struggle with due to the fixed parameters of converged policies. Hence, SRLM interprets real-time human feedback inference via an LLM

as high-level global information to guide low-level actions execution. This interactive framework not only enhances user experience but also boosts navigation performance.

Despite the significant applications of LLM in a wide range of areas, such as robotics [7], HRI [8], logical reasoning [9], [10], etc, the deployment of LLM-based social navigation planners is still limited by the gaps in navigation information (such as location and velocity) to language text and LLM's training dataset. Moreover, most recent LLM-based navigation systems [7], [11] directly generate macro-action functions rather than real low-level motion control instructions, due to the insensitivity and misunderstanding of LLM regarding continuous space's numerical values. To adapt the ability of large models in navigation aspects, SRLM designs a textual embedding encoder and a social navigation prompt to convert environmental information for generating low-level navigation actions directly.

Our goal is to develop an interactive social navigation artificial general intelligence aligned with each user's personal preferences. Additionally, we organically incorporate existing deep reinforcement learning-based SOTA navigation planners with LLM-based approaches into a large navigation model. This consideration arises from the challenge that recent LLM-based planners face in handling complex dynamic optimization problems in crowded environments. The main contributions of this paper can be summarized as follows:

- We propose SRLM, a human-in-loop interactive social robot navigation framework driven by LLMs and deep reinforcement learning (DRL). SRLM can execute personalized social robot tasks according to users' requests, preferences, and real-time feedback from human language, serving as an interactive social robot assistant.
- SRLM leverages an advanced DRL-based social planner and a language navigation model to generate socially compliant robot behaviors. Additionally, the language navigation model (LNM) memory mechanism can store temporal data and provide long-term evaluations and feedback to refine DRL-based and LLM-based social planners.
- SRLM adapts the properties of user tasks and personal preferences driven by LLM as high-level global guidance into reinforcement learning from human feedback (RLHF) modifications. In this setup, the reward network from RLHF can be further aligned by users rather than human training supervisors in the DRL-based planner.
- SRLM demonstrates robust and promising exhibitions of socially compliant behaviors in various experiments.

This material is based upon work supported by the National Science Foundation under Grant No. IIS-1846221. ¹SMART Laboratory, Department of Computer and Information Technology, Purdue University, West Lafayette, IN, USA. wang5716@purdue.edu, robotics.lemao@gmail.com, wang5357@purdue.edu, minb@purdue.edu.

II. BACKGROUND

LLM-driven Navigation. Inspired by the promising of LLM across a wide range of applications, successes driven by extensive computational resources and advanced machine learning methods have motivated massive research in robotics and HRI. For instance, [12] designs an LLM-driven mobile manipulator that offers services or infers user preferences from human language requests. The inference ability of LLM is essential for interactive social robots capable of tracking real-time user language feedback to adjust robot behaviors. Here, we leverage a high-level LLM block as an interactive framework to generate global guidance in response to human feedback.

Moreover, the context semantic inference of LLM can also be employed for navigation execution. For instance, [13] introduces LLM-guide visual language navigation, where planners are controlled by conclusions drawn from textual robot perception features provided by LLM. However, despite the reasonable evidences and dependencies for LLM in similar social navigation environments, the data schema and inference difficulty of social navigation are more complicated than those of visual or language navigation. Therefore, we abstract social navigation environmental features into textual data to adapt an LLM-driven large navigation model capable of inferring social interaction and directly generating low-level robot actions.

To further improve the inference ability, the chain-of-thoughts [9] technology has been developed to generate intermediate steps of inference process. The chain-type construction provides more generative information and an adjustable method. Additionally, structures such as trees and graphs have been proposed for a better inference structure, as seen in [10], [14]. Thus, considering the ephemeral limitations of LLM inference, particularly due to potential probabilistic illusions in LLM reasoning and the insensitivity of sequential floating-point numbers in LLM, the reinforcement learning navigation model (RLNM) is introduced to maintain baseline performance. This performance is adaptively fused by the large feedback model (LFM) via a Graph-of Thoughts (GoT) construction.

Socially Aware Robot Navigation. After early applications of robotics in social navigation society, such as MINERVA [15], socially aware robot navigation tasks are primarily conducted via decoupled and coupled strategies [16]. Decoupled approaches infer pedestrian motion intents and patterns to construct potential safe areas for planing. However, the separation of modeling and planning often overlooks potential cooperation, leading to the establishment of limited feasible spaces, known as the freezing robot problem [17], particularly with the increasing presence of humans. Alternatively, coupled approaches encode potential cooperation into navigation inference to address unwarranted ignorance.

On the other hand, explicitly coupled approaches are implemented through game theoretic planning [18], Gaussian processes [19], and topology analysis [3]. However, the challenge of optimization in highly dynamic environments

restricts the further deployment of conventional approaches [20] and explicitly coupled approaches, especially with the increasing complexity of the environment. Recently, the paradigm of cooperative collision avoidance has facilitated a set of promising works [2], [21], which implicitly approximate human-like navigation awareness and insight through advanced neural networks to encode potential human-robot cooperation and compliance with social norms into robot behavior. These neural networks are then trained using DRLs to iterate through different situations. For instance, efforts have been made in the development of neural network technologies for social navigation, such as attention mechanisms [22], graph construction [21], and transformers [2].

Despite aforementioned neural networks being utilized to evaluate underlying human-robot interaction and pedestrian intents for cooperative collision avoidance, human preferences are still not well represented. [23] incorporates the high-order uncertainty of human movements as pedestrian preference distributions into the social navigation planner based on variational analysis. Furthermore, the SAN task is also motivated by the direct involvement of human intelligence through RLHF in [2], [24], where human expectations and social norms are studied and embedded by a reward neural network to train the policy. More currently, [25] extends the learning-based planner in multi-robot scenarios.

Learning-based approaches generally exhibit benchmarking efficacy. However, the converged DRL policies often result in degradation, with limited generalization ability in unfamiliar scenes, and they are also difficult to adapt to real-time user feelings. Hence, we leverage LNM and LFM to improve the adaptability and robustness of DRL-base planners, incorporating the inference capability of large models for both real-time human feedback and low-level motion execution.

III. PRELIMINARY

SRLM is an interactive social navigation framework that understands user commands (e.g. “Pick up my bag to me”) and personal preferences (such as the user needing a larger privacy area with the robot) into a set of high-level instructions as global guidance from human language input. Herein, SRLM blends a high-level and low-level execution system, in which task objectives, such as point-to-point (P2P), human-guide (HG), human-follow (HF), user preferences (privacy distance), and social norm property (whether to wait each pedestrian), are composed into high-level global guidance for low-level robot action generation.

Subsequently, the pre-trained LNM and RLNM generate low-level robot actions with respect to textual or featurized HRI state presentations and the above global guidances. Moreover, the global guidance information can be modified or updated by real-time human feedback as well, such as when a user adds personal feelings or changes task objectives, prompting instructions to be replanned. Lastly, an additional feedback and memory mechanism is adapted to adjust LNM & RLNM incorporating behaviors from past trajectories. The real-time evaluation and feedback mechanism

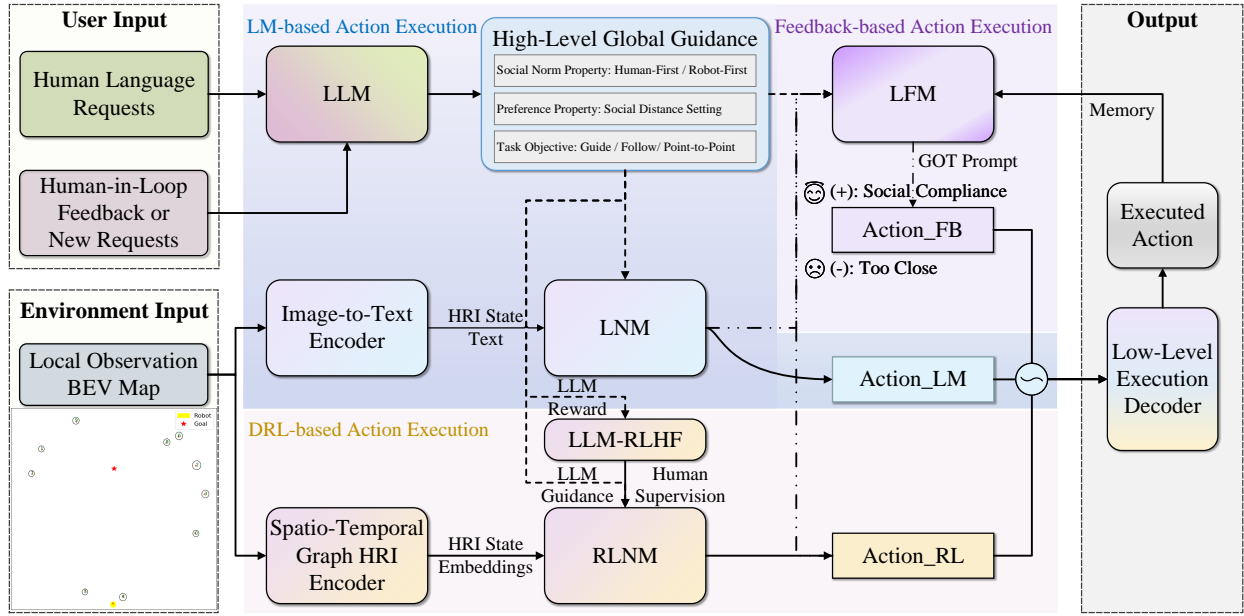


Fig. 1. SRLM architecture: SRLM is implemented as a human-in-loop interactive social robot navigation framework, which executes human commands based on LM-based planner, feedback-based planner, and DRL-based planner incorporating. Firstly, users' requests or real-time feedbacks are processed or replanned to high-level task guidance for three action executors via LLM. Then, the image-to-text encoder and spatio-temporal graph HRI encoder convert robot local observation information to features as LNM and RLNM input, which generate RL-based action, LM-based action, and feedback-based action. Lastly, the above three actions are adaptively fused by a low-level execution decoder as the robot behavior output of SRLM.

provide an adaptive heuristic to take their advantages. For instance, the DRL-based action execution model maintains a lower bound when the LM-based model encounters explicit mistakes or dangers, thus providing fundamental performance as the social navigation benchmark. On the other hand, the LM-based action execution model incorporates user personal modifications from user language to improve the robustness of DRL-based action execution model and RLHF reward network.

Herein, the interactive social robot navigation problem is formulated as a Dec-POSMDP (decentralized particularly observable semi-Markov decision process) problem based on [25], characterized by the tuple $\langle \mathcal{S}, \mathcal{U}, \mathcal{A}, \Omega, \mathcal{O}, \mathcal{P}, \mathcal{R}, \mathbf{R}, \mathcal{C}, \mathcal{S}_0, \gamma, \mathbf{N}, \Upsilon \rangle$. Here, $\mathbf{s}_t = [\mathbf{s}_t^r, \mathbf{s}_t^{h_1}, \dots, \mathbf{s}_t^{h_N}] \in \mathcal{S}$ denotes the fully observable and unobserved states of the robot and humans at the t -th timestep, belong to the state space, with the observable state denoted by $\mathbf{s}_t^o = [p_x, p_y, v_x, v_y, \rho]$ covering individual position, velocity, and radius information that can be estimated by the robot. Accordingly, pedestrians' personal preferences and intent goals remain unobserved by robots, represented as $\mathbf{s}_t^{uo} = [g_x, g_y, v_{pref}]$. Moreover, $\mathbf{u}_t \in \mathcal{U}$ represents robot macro-action (MA), such as waypoint locations or robot operations, which are adaptive to real-time user requirements or feedback, while robot local-action (LA) are denoted by $\mathbf{a}_t = [a_x, a_y] \subseteq \mathcal{A}$, representing acceleration. $\mathcal{O}(\mathbf{s}^o | (\mathbf{s}, \mathbf{a}))$ denotes the observation probability of the robot in the observation space Ω , and \mathcal{P} represents the state transition probability. \mathcal{R}, \mathbf{R} represent the MA reward and LA reward space separately, wherein the LA reward neural network r_φ is trained by the RLHF procedure. In particular, SRLM also introduces user commands as an additional large model reward r_{LM}

for LA reward (e.g., LLM designs a reward function term " $r_{LM} = -r_a | (dis_{r,i} < 2m)$ " corresponding to user language "Please maintain at least 2 m distance to me"). The MA reward is generated by the following objective: $\mathcal{R}(\mathbf{s}, \mathbf{u}) = \arg \max \mathbb{E}[\sum_{t=0}^T \gamma^t \mathbf{R}(\mathbf{s}_t, \mathbf{a}_t) | \mathbf{a}_t \sim \mathbf{u}]$. Additionally, \mathcal{C} represents the conditional function, which can be updated by user language comments from LLM, \mathcal{S}_0 is the initial distribution, \mathbf{N} is the number of pedestrians, $\gamma \in [0, 1]$ is a discount factor, and Υ denotes the LLM global guidances wherein task objectives, user preferences, and robot properties are involved.

The interactive social navigation task statement can be viewed as a condition of a single robot from the multi social robot navigation task definition [25], with the same robot kinematic and dynamic configurations. For further definitions and theorems, refer to [25], [26].

IV. METHODOLOGY

SRLM leverages multiple LLM-based large models and a DRL-based model to provide interactive social robotic services with respect to users' requirements or feedback. In this framework, the LLM-based large model (LNM) and DRL-based approach (RLNM) are adaptively incorporated with an LLM-based evaluation model (LFM), as shown in Fig 1.

A. Human-in-Loop Interactive Mechanism

SRLM drives social robots through a high-level guidance and low-level execution incorporation strategy. Firstly, LLM handles user language input to capture semantic features for global guidance generation. We define three typical social robot tasks (P2P, HG, HF). In the HG task, the social robot navigates to a target point while also maintaining a limited distance with the user until reaching the target location.

LNM Prompt:

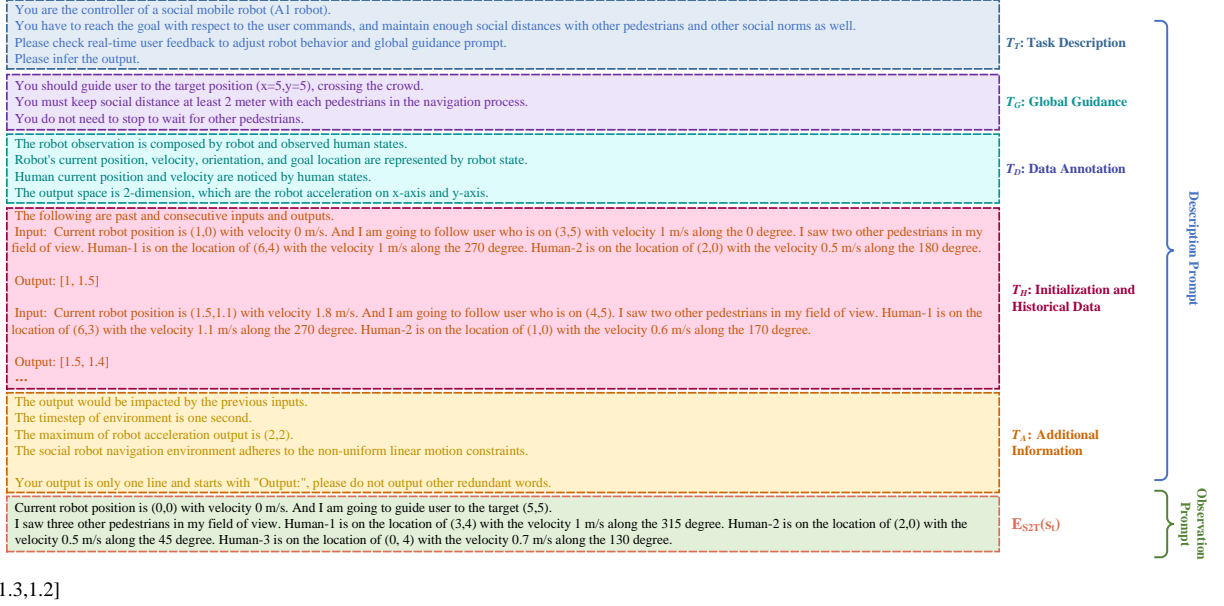


Fig. 2. An illustration of LNM: The prompt engineering of LNM comprises task description, global guidance, data annotation, initialization, historical data, additional information, and encoded state to directly generate low-level robot actions $[a_x, a_y]$. Please zoom in on the images for details.

For the HF task, the robot's target is updated by the user's real-time location, and the robot must ensure that the user is within its field of view (FOV) at a comfortable social distance. The basic P2P task involves simply assigning a new target to robot. Moreover, social norm attributes are considered, such as pedestrian-first or robot-first, where the robot will come to a full stop when a pedestrian appears within a fixed distance (d_s) area under the condition of pedestrian-first. Additionally, user personal preference attributes are collected to select different styles of DRL policy networks in RLNM. Here, we trained three pre-trained policy networks with preferences for large, moderate, and minimal social distance.

Subsequently, global guidances T_G are further employed in the following low-level execution blocks: LNM, RLNM, and LFM, where global guidance is described in the prompt engineering of LNM and LFM to supervise LM-based and FB-based action execution. RLNM encodes the target and personal attributes into Υ , which can modify the conditional function \mathcal{C} and select the preferred policy network.

Additionally, the LLM block can modify the global guidance or replan new global information based on real-time user feedback or new requests. The human-in-loop interactive mechanism enhances the robustness and flexibility of SRLM, allowing users to adjust robot behaviors based on their feelings during the real-time execution process. For example, if the robot is too closed to pedestrians, users can provide personal feedback to modify the robot's social distance to a larger value.

B. Language Navigation Model

LNM adapts LLM's supervising ability of context semantic inference to drive a social robot as a low-level motion controller in a human-filled environment. Due to the

current requirement of textual information input by LLM, the perception information of the social robot (such as the position of pedestrians) have to be converted into textual information via an image-to-text encoder. Here, the image-to-text encoder translates the robot's observation state into text descriptions, which mainly include the location and velocity of the robot and observed pedestrians, as well as other features such as orientation and personal radius. However, simply feeding the robot's observation and action pairs into LLM cannot produce a robust controlling sequence, due to the insensitivity and misunderstanding of LLM regarding a set of numeric values. To enhance the LLM's inference ability on temporal series, SRLM also implements the prompt engineering T_{HRI} , which consists of the following parts: task description T_T , global guidance T_G , data annotation T_D , initialization and historical data T_H , and additional information T_A , as shown in Fig. 2.

Firstly, task description T_T is a paragraph that explains the environment configuration and robot properties. The global guidance T_G notes immediate task objectives, user personal preference requirements, and social norm conditions, which are abstracted from the output of the first LLM block. The third subsection is data annotation T_D , which specifies the implications and data formulation of inputs and outputs. The demonstration data or executed actions are saved into initialization and historical data T_H . Finally, additional information T_A provides supplementary information.

In the execution process, the initialization textual information from demonstrations is saved in first several time steps after the robot receives user commands, and then the demonstration data will be replaced with historical data by a memory mechanism.

$$\begin{aligned} T_{HRI} &= f[E_{S2T}(s_t), LLM(Requests)] \\ \mathbf{a}^{LM} &= LNM(T_{HRI}) \end{aligned} \quad (1)$$

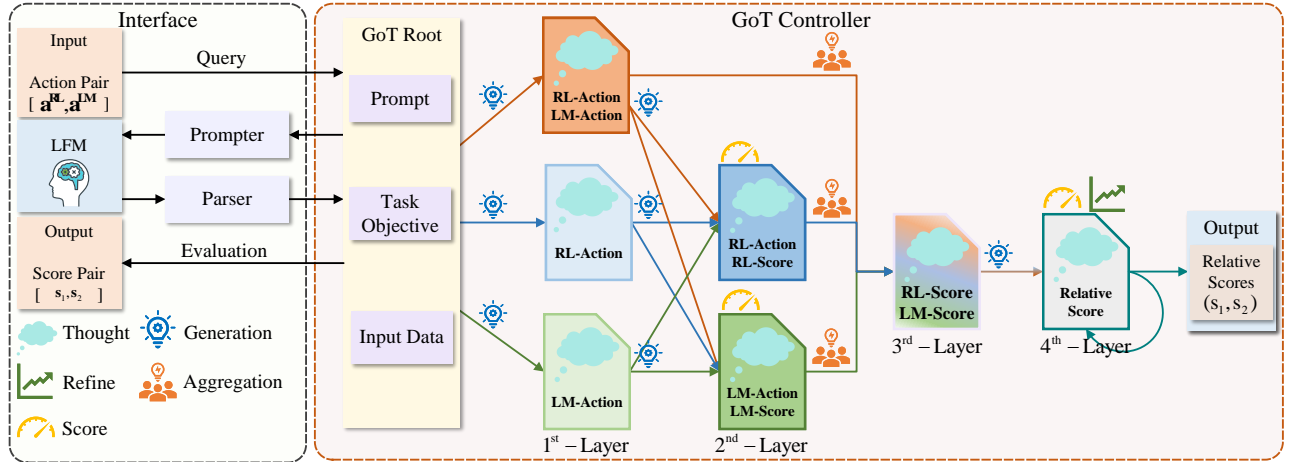


Fig. 3. LFM framework: LFM reconciles the output from LNM \mathbf{a}^{LM} and RLNM \mathbf{a}^{RL} to stabilize final mixture action \mathbf{a}^R , in which the GoT construction of LFM is designed to evaluate and score the above two executions with more generated evidences or intermediate steps chains from different perspectives.

C. Language Feedback Model

SRLM employs the ability of contextual understanding and inference in LNM to enhance the adaptability of RLNM, aligning and tailoring the pre-trained DRL policy with different personal preferences and task objectives. Therefore, the integration of DRL-based planner and LM-based planner is facilitated by the LFM, which evaluates both actions and estimates their relative weights as follows:

$$s_1, s_2 = LFM(\mathbf{a}^{RL}, \mathbf{a}^{LM}, \mathbf{a}^M, T_{HRI} \parallel \mathcal{G}_{GOT}) \quad (2)$$

where \mathbf{a}^M is a set of executed actions from the memory buffer, and \mathcal{G}_{GOT} is the graph of thought prompting of LFM.

The critical part of LFM is the GoT prompting technique [10]. GoT generates and illustrates intermediate reasoning steps as vertices to significantly improve the comprehensibility and inference performance of LFM. Despite requiring additional information and resources, the final inference can be supported more thoroughly with diversified evidence and threads. Moreover, the graph construction also addresses the stochasticity of the inference process through interpretations from multiple reasoning paths.

As shown in Fig. 3, a directed graph framework $\mathcal{G}_{GoT} = \{\mathcal{V}, \mathcal{E}\}$ is designed in LFM, in which vertices present solutions in different aspects. Thoughts' transformations or correlations are captured by edges where generation, aggregation, refining, and scoring are typically involved. The aggregation operation is defined as $[\mathcal{V}^+ = \{V^+\}; \mathcal{E}^+ = \{(V_1, V^+), \dots, (V_k, V^+)\}]$, generation operation is $[\mathcal{V}^+ = \{V_1^+, \dots, V_{k'}^+\}; \mathcal{E}^+ = \{(V, V_1^+), \dots, (V, V_{k'}^+)\}]$, and the refining operation can be presented as $[\mathcal{V}^+ = \phi; \mathcal{E}^+ = \{(V, V)\}]$. Additionally, the scoring thought is calculated as $\mathcal{E}(V, \mathcal{G}_{sub}, f_{LM})$, where \mathcal{G}_{sub} is a subgraph of \mathcal{G}_{HRI} or the whole graph, and f_{LM} is a pre-trained large model.

The LFM's GoT queries the action pairs a^{RL} and a^{LM} as input with the prompt engineering of LNM and a new objective description. Then, a^{RL} , a^{LM} , and $a^{RL} \& a^{LM}$ respectively are fed into the next three different vertices via generation edges. Subsequently, a^{RL} and a^{LM} are further evaluated and generated via the first-layer three thoughts to

score individual actions as (s_1^i, s_2^i) . After the first individually evaluation, the 3rd-layer vertex is aggregated by two 2nd-layer thoughts and the 1st-layer a^{RL} and a^{LM} thoughts to incorporate individual action scores. Finally, the 3rd-layer vertex generates the relative score thought, which is refined to calculate the combinational scores (s_1, s_2) .

D. Reinforcement Learning Navigation Model

Although LNM adapts the remarkable ability of HRI understanding into navigation decision-making, independent LNM still struggles with uncertainty and the infeasibility of decision-making in complex dynamic environments with continuous space. In contrast, DRL-based RLNM leverages a convergent and efficient policy to address these issues as observed in many works [2], [21], [25]. Therefore, inspired by [2], the DRL-based action execution is employed in SRLM with an ST-graph HRI encoder, LLM-RLHF block, and RLNM block.

RLNM implicitly models the surrounding long-term environmental dynamics to demonstrate socially acceptable navigation behaviors in human-filled environments, based on a hybrid spatial-temporal transformer \mathcal{F}_{Trans} from current SOTA social navigation benchmark NaviSTAR [2]. Firstly, the underlying human intents and spatial-temporal dependencies are captured by a spatial-temporal transformer framework. Subsequently, the heterogeneous features mentioned above are fused through a multimodal transformer fusion network. Hence, the environmental dynamics of the social navigation scenario, denoted as \mathbf{X}_E , are constructed as an ST-graph (spatio-temporal graph) \mathcal{G}_{ST} from robot local observations as follows:

$$\mathbf{X}_E = \mathcal{F}_{NaviSTAR}(s_1, \dots, s_t \parallel \mathcal{G}_{ST}) \quad (3)$$

Additionally, the RLHF block is developed to exhibit socially compliant robot behaviors based on [27], encoding human intelligence and supervision in the policy training procedure. For policy training, two different random segments (σ_1, σ_2) are displayed to human supervisors at once. Then, human supervisors must label the segment pair with personal preference ω as $(\sigma_1, \sigma_2, \omega)$ into the data buffer, which is

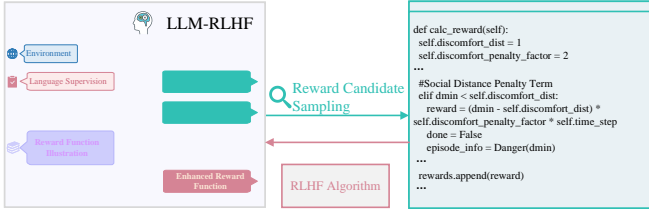


Fig. 4. LLM-RLHF block: The LLM is introduced in our RLHF training procedure to effectively interpret human supervision from language feedback, wherein the reward functions are generated directly.

utilized to update the reward neural network r_ϕ and the robot policy π . Lastly, the NaviSTAR [2] planner is developed by RLNM to address interactive social navigation tasks as a Dec-POSMDP paradigm, in which it generates macro-action \mathbf{u}^{RL} and local-action \mathbf{a}^{RL} based on HRI latent embedding \mathbf{X}_E as follows:

$$\mathbf{u}^{\text{RL}}, \mathbf{a}^{\text{RL}} \sim \mathcal{RLNM}(\mathbf{X}_E) \quad (4)$$

To understand human intents and preferences directly from language, SRLM designs an adaptive reward function r_{LM} to enhance the LLM-RLHF training procedure based on [28], [29], which is incorporated with the RLHF reward neural network r_ϕ to improve the robustness of the DRL-based action executor. As shown in Fig. 4, the environmental programming specification and personal preference are provided as context prompt engineering to generate the LM reward function corresponding to existing programming formulation and supervisor preference.

Although many DRL-based social navigation approaches [2], [21], [22], [25] demonstrate excellent performance benchmarks for SAN tasks in latent HRI inference and social compliance collision avoidance, the learning algorithms are limited and constrained by training conditions and biased policy patterns. This limitation makes it difficult to maintain sufficient performance in general application scenarios. Hence, a low-level execution decoder is employed to fine-tune the DRL-based planner using the relative weights (s_1, s_2) from LFM and the LNM action \mathbf{a}^{LM} as follows:

$$\mathbf{a}_t^{\text{R}} = \text{Decoder}(s_1 \cdot \mathbf{a}_t^{\text{RL}} + s_2 \cdot \mathbf{a}_t^{\text{LM}}) \quad (5)$$

V. EXPERIMENTS AND RESULTS

A. Simulation Experiment

1) *Simulation Setup*: We conducted simulation experiments to evaluate the performance of our approach and other ablation models. We developed a human-in-loop interactive social robot navigation environment based on a gym social navigation simulator [2], [25]. In comparison with the original simulator version, user real-time language commands and feedback can be directly implemented to adjust robot behaviors during execution, where both large model blocks (LLM, LNM, and LFM) are configured by GPT-4 [30]. However, the kinematics, dynamics, and other environmental constraints remain the same as in previous works [25].

The default scenario of our experiments involves a robot assisting a user who can talk with robot in real-time, in

navigating to a target in an open space among several pedestrians, all simulated by the ORCA policy [20]. There are three main interactive task types in the simulation: human-guiding, human-following, and point-to-point. In the human-guiding task, the social robot guides the user to the target with a physical ribbon connection, necessitating that the robot must maintain a larger space with other pedestrians. The robot must maintain a suitable distance from the user until the user reaches the destination. The P2P task is the same as in previous simulations, with the target potentially changing halfway through the task based on the user's real-time command.

All approaches were trained with 1×10^4 episodes and tested with 500 random cases for each task, conducted on a desktop with an Intel i9-13900k CPU and an Nvidia 4090 GPU. In each training or testing epoch, a human language requests generator was designed to publish task objectives with personal preferences. Particularly, real-time feedback is stochastically established from the generator with a 50% probability halfway through the current task to update the robot's goal, user preferences, or other attributes.

2) *Baselines and Ablation Models*: As shown in Table I, we have set up a comparison of our algorithm with five other baselines or ablation models as follows: (1) A traditional navigation strategy ORCA [20] is utilized as the basic planner, wherein only the global LLM block is maintained to understand high-level human commands for task target establishments; (2) We implement CADRL [31] as the baseline for learning-based approaches, in which the LLM block is also employed for interactive navigation; (3) For the second ablation model, LNM and LFM are detached inside to test the performance of RLNM as SR-RLNM; (4) RLNM and LFM are removed to be viewed as the first ablation model, where the robot is driven only from LNM output as SR-LNM; and (5) For the final one, LFM is replaced by a fixed relative parameter pair (0.5 & 0.5) as SR-LFM.

3) *Evaluation Metrics*: As shown in Fig. 5 and Table I, all methods have been evaluated using 500 random test cases for each task (total 1500 cases) individually, with two evaluation metrics: successful rate (SR) and social score (SS) [2]. The SS metric considers various social navigation performance factors such as travel time, collision rate, success rate, discomfort level, and etc.

TABLE I: SIMULATION EXPERIMENT RESULTS

Methods	Success Rate				Social Score			
	Task Type				Task Type			
	P2P	HG	HF	AVG	P2P	HG	HF	AVG
ORCA [20]	43	21	20	28	35	18	24	26
CADRL [31]	64	47	52	54	58	52	55	55
SR-RLNM	92	78	77	81	83	67	65	70
SR-LNM	54	69	71	65	48	52	58	54
SR-LFM	89	82	84	85	88	74	72	78
SRLM	94	95	93	94	97	93	95	95

4) *Quantitative Measurement*: Firstly, we analyze the ability of each planner in terms of average trajectory quality with SR and SS metrics. The SR and SS statistic box plots of each planner are shown in Fig. 5. SRLM demonstrates 94% SR and 95 SS ($\mu = 95$, $\sigma = 1.85$) higher than

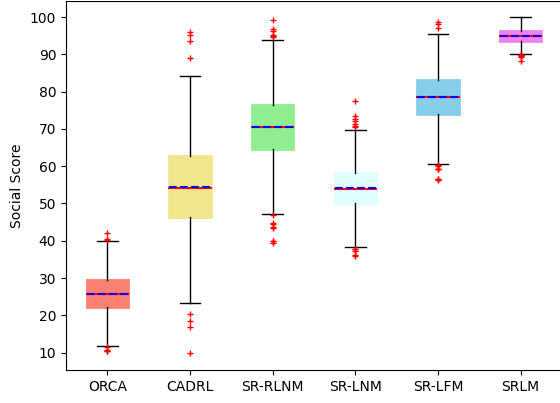


Fig. 5. The box plot of social score SS.

others. Then, we conducted an ANOVA tests on SR and SS metrics to examine following hypotheses: ($H_0^{SR}: \mu_1 = \mu_2 = \dots = \mu$), where SR null hypothesis H_0^{SR} claims that SR is independent of the selection of planners, and ($H_1^{SR}: \exists \mu_i \neq \mu; i \in [0, \#A]$), where the SR alternative hypothesis states that there exists a significant difference among algorithms. Similarly, the hypotheses for SS are defined as follows: (SS null hypothesis $H_0^{SS}: \mu_1 = \mu_2 = \dots = \mu$), (SS alternative hypothesis $H_1^{SS}: \exists \mu_i \neq \mu; i \in [0, \#A]$).

The linear mixed-effects model is introduced to test the relationship between experimental conditions and objectives in the ANOVA. The ANOVA revealed significant variance among the conditions of planner selection, resulting in a p-value < 0.05 and an F-value of 15410.139 as shown in Table II. Overall, the hypotheses (H_1^{SR}, H_1^{SS}) are confirmed, while (H_0^{SR}, H_0^{SS}) are rejected. In other words, the condition of planner selection is a significant factor in navigation performance. Specifically, as shown in Table I and Fig. 5, we observe that SRLM generates the best trajectory for social robot navigation compared to other strategies. The expected means and confidence intervals for all criteria of each planner are summarized by Fig. 5.

TABLE II: SOCIAL SCORE ANOVA TABLE

	Sum Sq	df	Mean Sq	F-value	p-value
Planner	4280451.552	5	856090.310	15410.139	< 0.0001
Error	499650.014	8994	55.554		
Total	4780101.566	8999			

5) *Effectiveness of LNM*: From Fig. 5, the ablation model SR-RLNM achieves a 90% SR and 90 SS, which is slightly lower than the performance of SRLM overall. We can observe that SR-RLNM can provide a benchmark performance derived from the RLNM capability. However, as shown in Fig. 6, SR-RLNM demonstrates a similar path quality to SRLM in the early timesteps, but SR-RLNM still adheres to previous strategic preferences even after receiving renovation feedback from the user updating the task objective and personal preference. Hence, the introduction of LNM in SRLM stabilizes the robustness of navigation performance, especially for the stage after user feedback, because the pre-trained DRL-based policy cannot adjust itself to highly adaptive behavioural representations in the execution stage.

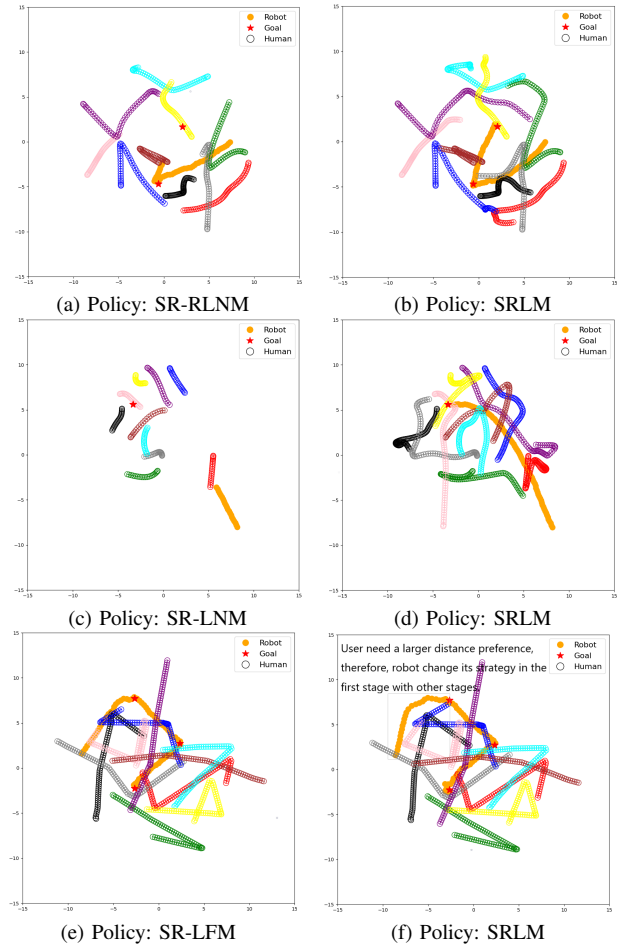


Fig. 6. Comparison of trajectory visualization: Visualization of trajectories for ablation models and SRLM, all tested using the same test case.

6) *Effectiveness of RLNM*: Despite the amazing inference ability exhibited by large language models in many applications, LLM-based developments of sequential control systems have struggled with highly dynamic environments and sequential data dimensions. The environments of social navigation tasks require robots to understand potential pedestrian intents and engage in HRI cooperation to adapt to environmental dynamics. Such challenges, coupled with the lack of RLNM compared to SRLM, result in struggling and precarious effects in dynamic scenarios. From both the average results and trajectory instances shown Fig. 6, we observe that SR-LNM exhibits many instances of reciprocal dance phenomena, where the robot swings from side to side. Thus, to maintain benchmarking performance for LLM-based social robots in dynamic spaces, we recommend continued use of DRL-based robot executors.

7) *Effectiveness of LFM*: As observed in Fig. 5 and Fig. 6, we find that SR-LFM exhibits limited planner capability compared to SRLM. The blunt fusion with fixed relative weights presents lower flexibility than LFM, because the LLM-driven LFM can infer the situation for a better fusion strategy from more evidence chains with the developments of GoT. The blending mechanism of LFM is significant

for adjusting and fusing two robot actions, leveraging the inference ability from LLM, which can effectively improve overall performance.

VI. CONCLUSION

In this work, we developed an interactive social robot large model. SRLM leverages the inference ability of LLM to interpret user language commands and enhance the adaptability of DRL-based navigation policy. Additionally, the GoT is developed by LFM to evaluate the relative action score of the executed actions from LLM-based and DRL-based planners, incorporating LNM and RLNM blocks. Finally, SRLM demonstrates outstanding efficiency compared to baselines and ablation models in both simulation and real-world experiments. Future work includes exploring its use in real-world robot applications.

REFERENCES

- [1] F. Yuan, M. Boltz, D. Bilal, Y.-L. Jao, M. Crane, J. Duzan, A. Bahour, and X. Zhao, "Cognitive exercise for persons with alzheimer's disease and related dementia using a social robot," *IEEE Transactions on Robotics*, 2023.
- [2] W. Wang, R. Wang, L. Mao, and B.-C. Min, "Navistar: Socially aware robot navigation with hybrid spatio-temporal graph transformer and preference learning," in *2023 IEEE/RSJ International Conference on Intelligent Robots and Systems (IROS)*, 2023, pp. 11 348–11 355.
- [3] C. I. Mavrogiannis and R. A. Knepper, "Multi-agent path topology in support of socially competent navigation planning," *The International Journal of Robotics Research*, vol. 38, no. 2-3, pp. 338–356, 2019.
- [4] C. Mavrogiannis and R. A. Knepper, "Hamiltonian coordination primitives for decentralized multiagent navigation," *The International Journal of Robotics Research*, vol. 40, no. 10-11, pp. 1234–1254, 2021.
- [5] P. Trautman, J. Ma, R. M. Murray, and A. Krause, "Robot navigation in dense human crowds: Statistical models and experimental studies of human-robot cooperation," *The International Journal of Robotics Research*, vol. 34, no. 3, pp. 335–356, 2015.
- [6] G. Manor, J. Z. Ben-Asher, and E. Rimon, "Time optimal trajectories for a mobile robot under explicit acceleration constraints," *IEEE Transactions on Aerospace and Electronic Systems*, vol. 54, no. 5, pp. 2220–2232, 2018.
- [7] D. Shah, M. R. Equi, B. Osiński, F. Xia, B. Ichter, and S. Levine, "Navigation with large language models: Semantic guesswork as a heuristic for planning," in *Conference on Robot Learning*. PMLR, 2023, pp. 2683–2699.
- [8] B. Li, P. Wu, P. Abbeel, and J. Malik, "Interactive task planning with language models," *arXiv preprint arXiv:2310.10645*, 2023.
- [9] J. Wei, X. Wang, D. Schuurmans, M. Bosma, F. Xia, E. Chi, Q. V. Le, D. Zhou *et al.*, "Chain-of-thought prompting elicits reasoning in large language models," *Advances in Neural Information Processing Systems*, vol. 35, pp. 24 824–24 837, 2022.
- [10] M. Besta, N. Blach, A. Kubicek, R. Gerstenberger, L. Gianinazzi, J. Gajda, T. Lehmann, M. Podstawski, H. Niewiadomski, P. Nyczyk *et al.*, "Graph of thoughts: Solving elaborate problems with large language models," *arXiv preprint arXiv:2308.09687*, 2023.
- [11] D. Shah, B. Osiński, S. Levine *et al.*, "Lm-nav: Robotic navigation with large pre-trained models of language, vision, and action," in *Conference on Robot Learning*. PMLR, 2023, pp. 492–504.
- [12] J. Wu, R. Antonova, A. Kan, M. Lepert, A. Zeng, S. Song, J. Bohg, S. Rusinkiewicz, and T. Funkhouser, "Tidybot: Personalized robot assistance with large language models," in *2023 IEEE/RSJ International Conference on Intelligent Robots and Systems (IROS)*, 2023, pp. 3546–3553.
- [13] W. Huang, P. Abbeel, D. Pathak, and I. Mordatch, "Language models as zero-shot planners: Extracting actionable knowledge for embodied agents," in *International Conference on Machine Learning*. PMLR, 2022, pp. 9118–9147.
- [14] G. Feng, B. Zhang, Y. Gu, H. Ye, D. He, and L. Wang, "Towards revealing the mystery behind chain of thought: A theoretical perspective," in *Thirty-seventh Conference on Neural Information Processing Systems*, 2023.
- [15] S. Thrun, M. Bennewitz, W. Burgard, A. B. Cremers, F. Dellaert, D. Fox, D. Hahnel, C. Rosenberg, N. Roy, J. Schulte *et al.*, "Minerva: A second-generation museum tour-guide robot," in *Proceedings 1999 IEEE International Conference on Robotics and Automation (Cat. No. 99CH36288C)*, vol. 3. IEEE, 1999.
- [16] C. Mavrogiannis, F. Baldini, A. Wang, D. Zhao, P. Trautman, A. Steinfield, and J. Oh, "Core challenges of social robot navigation: A survey," *ACM Transactions on Human-Robot Interaction*, vol. 12, no. 3, pp. 1–39, 2023.
- [17] P. Trautman, J. Ma, R. M. Murray, and A. Krause, "Robot navigation in dense human crowds: Statistical models and experimental studies of human-robot cooperation," *The International Journal of Robotics Research*, vol. 34, no. 3, pp. 335–356, 2015.
- [18] W. Schwarting, A. Pierson, S. Karaman, and D. Rus, "Stochastic dynamic games in belief space," *IEEE Transactions on Robotics*, vol. 37, no. 6, pp. 2157–2172, 2021.
- [19] P. Trautman and K. Patel, "Real time crowd navigation from first principles of probability theory," in *Proceedings of the international conference on automated planning and scheduling*, vol. 30, 2020, pp. 459–467.
- [20] J. Van Den Berg, S. J. Guy, M. Lin, and D. Manocha, "Reciprocal n-body collision avoidance," in *Robotics Research: The 14th International Symposium ISRR*. Springer, 2011, pp. 3–19.
- [21] S. Liu, P. Chang, Z. Huang, N. Chakraborty, K. Hong, W. Liang, D. L. McPherson, J. Geng, and K. Driggs-Campbell, "Intention aware robot crowd navigation with attention-based interaction graph," in *2023 IEEE International Conference on Robotics and Automation (ICRA)*. IEEE, 2023, pp. 12 015–12 021.
- [22] C. Chen, Y. Liu, S. Kreiss, and A. Alahi, "Crowd-robot interaction: Crowd-aware robot navigation with attention-based deep reinforcement learning," in *2019 international conference on robotics and automation (ICRA)*. IEEE, 2019, pp. 6015–6022.
- [23] M. Sun, F. Baldini, P. Trautman, and T. Murphey, "Move Beyond Trajectories: Distribution Space Coupling for Crowd Navigation," in *Proceedings of Robotics: Science and Systems*, Virtual, July 2021.
- [24] R. Wang, W. Wang, and B.-C. Min, "Feedback-efficient active preference learning for socially aware robot navigation," in *2022 IEEE/RSJ International Conference on Intelligent Robots and Systems (IROS)*. IEEE, 2022, pp. 11 336–11 343.
- [25] W. Wang, L. Mao, R. Wang, and B.-C. Min, "Multi-robot cooperative socially-aware navigation using multi-agent reinforcement learning," *arXiv preprint arXiv:2309.15234*, 2023.
- [26] S. Omidshafiei, A.-A. Agha-Mohammadi, C. Amato, S.-Y. Liu, J. P. How, and J. Vian, "Decentralized control of multi-robot partially observable markov decision processes using belief space macro-actions," *The International Journal of Robotics Research*, vol. 36, no. 2, pp. 231–258, 2017.
- [27] K. Lee, L. Smith, A. Dragan, and P. Abbeel, "B-pref: Benchmarking preference-based reinforcement learning," in *Thirty-fifth Conference on Neural Information Processing Systems Datasets and Benchmarks Track (Round 1)*, 2021.
- [28] M. Kwon, S. M. Xie, K. Bullard, and D. Sadigh, "Reward design with language models," in *The Eleventh International Conference on Learning Representations*, 2022.
- [29] Y. J. Ma, W. Liang, G. Wang, D.-A. Huang, O. Bastani, D. Jayaraman, Y. Zhu, L. Fan, and A. Anandkumar, "Eureka: Human-level reward design via coding large language models," *arXiv preprint arXiv:2310.12931*, 2023.
- [30] –, "Gpt-4 technical report," *arXiv preprint arXiv:2303.08774*, 2023.
- [31] Y. F. Chen, M. Everett, M. Liu, and J. P. How, "Socially aware motion planning with deep reinforcement learning," in *2017 IEEE/RSJ International Conference on Intelligent Robots and Systems (IROS)*. IEEE, 2017, pp. 1343–1350.